

Boosting drug-disease association prediction for drug repositioning via dual-feature extraction and cross-dual-domain decoding

Enqiang Zhu^a, Xiang Li^a, Chanjuan Liu^{b,*} and Nikhil R. Pal^c

^a*Institute of Computing Science and Technology, Guangzhou University, Guangzhou, 510006, China*

^b*School of Computer Science and Technology, Dalian University of Technology, Dalian, 116024, China*

^c*Electronics and Communication Sciences Unit, Indian Statistical Institute, Calcutta, India*

ARTICLE INFO

Keywords:

Drug Repositioning
Deep Learning
Self-attention
Feature Extraction
Cross-dual-domain

ABSTRACT

Uncovering new therapeutic uses of existing drugs, drug repositioning offers a fast and cost-effective strategy and holds considerable significance in the realm of drug discovery and development. In recent years, deep learning techniques have emerged as powerful tools in drug repositioning due to their ability to analyze large and complex datasets. However, many existing methods focus on extracting feature information from nearby nodes in the network to represent drugs and diseases, without considering the potential inter-relationships between the features of drugs and diseases, which may lead to inaccurate representations. To address this limitation, we use two features (similarity and association) to capture the potential relationships between the features of drugs and diseases, proposing a Dual-Feature Drug Repositioning Neural Network (DFDRNN) model. DFDRNN uses a self-attention mechanism to extract neighbor features and incorporates two dual-feature extraction modules: the intra-domain dual-feature extraction (IntraDDFE) module for extracting features within a single domain (drugs or diseases) and the inter-domain dual-feature extraction (InterDDFE) module for extracting features across domains. By utilizing these modules, we ensure more appropriate encoding of drugs and diseases. Additionally, a cross-dual-domain decoder is designed to predict drug-disease associations in both domains. Our proposed DFDRNN model outperforms six state-of-the-art methods on four benchmark datasets, achieving an average AUROC of 0.946 and an average AUPR of 0.597. Case studies on two diseases show that the proposed DFDRNN model can be applied in real-world scenarios, demonstrating its significant potential in drug repositioning.

1. Introduction

In the field of medicine, drug development is a complex and time-consuming process. It involves three main stages: the discovery stage, the preclinical stage, and the clinical stage. This process typically takes 10-15 years and around \$2.8 billion on average (Fisher Wilson, 2006; Vijayan et al., 2022). Despite continuous efforts and innovation, the traditional drug development model faces significant risks and sometimes leading to the termination of projects due to concerns about drug efficacy, safety, or commercial viability. Notably, a high proportion (80-90%) of these projects fail during clinical trials (Vijayan et al., 2022; Di-Masi et al., 2010). Therefore, finding a more efficient and precise method for drug development is critically important and valuable.

Computational drug repositioning is a powerful strategy that aims to discover alternative uses of already approved drugs taking into account their potential side effects (Dudley et al., 2011; Wang et al., 2024). This approach uses computational and bioinformatics tools and is more efficient and cost-effective than traditional drug research and development methods. It allows for rapid screening of numerous candidate drugs and accelerates the development of new therapeutic options. Repurposing existing drugs can significantly reduce development costs compared to developing new drugs from

scratch. In response to new health crises, such as pandemics, repurposing known drugs can provide a quicker response compared to developing new treatments. This method can also identify new usage for drugs that may be effective for diseases lacking effective treatments and thereby addressing significant health challenges.

Machine learning is commonly used in computational drug repositioning. Traditional techniques like random forest (RF), support vector machine (SVM), and decision trees are often applied for this purpose (Cai et al., 2023). For instance, Peng et al. (2017) introduced a novel drug-target interaction screening framework called PUDTI, which utilized SVM to identify potential drug repositioning targets. Shi et al. (2019) proposed a method for predicting drug-target interactions using Lasso dimensionality reduction and a random forest classifier. Zhao et al. (2022) and Yang et al. (2023) employed random forests in their final prediction step, while other techniques such as decision trees (Xuan et al., 2019), matrix factorization (Yang et al., 2021; Luo et al., 2018; Sadeghi et al., 2022), and logistic regression (Yu et al., 2020) have also been developed.

In recent years, deep learning technology has become a powerful tool in bioinformatics, as evidenced by (Zhang et al., 2017; Mahdaddi et al., 2021; Bansal et al., 2024). Unlike traditional machine learning methods, deep learning technology can effectively capture high-level hidden representation using deep architectures without manual feature selection and tuning (Yu et al., 2022). Existing deep learning methods for drug repositioning often incorporate

*Corresponding author

 zhuenqiang@gzhu.edu.cn (E. Zhu); 1x160@gzhu.edu.cn (X. Li); chanjuanliu@dlut.edu.cn (C. Liu); nrpa159@gmail.com (N.R. Pal)

graph neural networks like Graph Convolutional Networks (GCN) and Graph Attention Networks (GAT) to for model building (Yu et al., 2021; Cai et al., 2021; Sun et al., 2022; Tang et al., 2023; Zhang et al., 2024). For instance, Yu et al. (2021) performed graph convolution operations on the drug-disease heterogeneous network to encode drugs and diseases, but did not account for the differences in encoding from different network spaces. Cai et al. (2021) distinguished between intra-domain and inter-domain feature extraction on the drug-disease heterogeneous network for encoding drugs and diseases. Zhang et al. (2024) extracted features of drugs and diseases from multiple neighborhood spaces and designed a contrastive learning loss to fuse these features. However, these studies did not consider the calculation of information weights from different neighbors. Authors in (Gu et al., 2022; Meng et al., 2024; Huang et al., 2024) used graph attention networks (GAT) to calculate the weights of neighbor aggregation and extract key neighbor information for encoding. Most deep learning models have so far been focused on extracting valuable features from neighborhoods. However, these models often employ single encoding approach and lack intentional encoding and decoding processes for association prediction. This can lead to the introduction of a large amount of noisy information during model training, resulting in the imprecise encoding of drugs and diseases, ultimately affecting the accuracy of prediction results.

In order to address this challenge, we propose a Dual-Feature Drug Repositioning Neural Network (DFDRNN) model that uses two features, similarity, and association, to accurately represent drugs and diseases. In comparison to existing methods, the proposed model incorporates two dual-feature extraction modules: the IntraDDFE module for extracting features within a single domain (drug or disease) and the InterDDFE module for extracting features across domains. DFDRNN uses a self-attention mechanism (SAM) to dynamically adjust the attention level of each input element to neighbor information, providing fine-grained weight allocation. This allows for efficient aggregation of neighbors and enhances the model's predictive power. Additionally, a cross-dual-domain decoder is designed to predict drug-disease associations in both domains. The key contributions of this paper are:

(1) To predict potential associations between drugs and diseases, we propose a dual-feature drug repositioning neural network (DFDRNN) model. A self-attention mechanism is used capture complex relationship among adjacent nodes. The encoder of DFDRNN consists of two dual-feature extraction modules: the intra-domain dual-feature extraction (IntraDDFE) module and the inter-domain dual-feature extraction (InterDDFE) module.

(2) The IntraDDFE module and InterDDFE module extract features exploiting information within a single domain and across domains, respectively, and track the dynamic changes of dual-feature to realize precise encoding of drugs and diseases.

Table 1
The statistics of the four datasets used in this study

Datasets	No. of drugs	No. of disease	No. of associations
Fdataset	593	313	1933
Cdataset	663	409	2532
Ldataset	269	598	18416
LRSSL	763	681	3051

(3) A cross-dual-domain decoder is proposed to perform cross-computation between two encoded features. This process yields decoding results for both the drug and disease domains, which help effectively predicting the drug-disease associations.

(4) The performance of the proposed method is compared with that of six state-of-the-art methods on four benchmark datasets. The experimental results show that DFDRNN outperforms other models. In addition, case studies on Alzheimer's and Parkinson's diseases validated the reliability of DFDRNN in practical applications.

The remainder of this paper is organized as follows. Section 2 describes the datasets and methods, detailing the implementation process of DFDRNN; Section 3 clarifies the experimental design and analyzes the experimental results, and Section 4 concludes this work with future research directions.

2. Materials and Methods

2.1. Datasets

We conducted experiments on four benchmark datasets. The first dataset, Fdataset (Gottlieb et al., 2011), includes 593 drugs from DrugBank (Knox et al., 2024) and 313 diseases listed in the Online Mendelian Inheritance in Man (OMIM) (Hamosh et al., 2005) database, comprising 1933 drug-disease associations. The second dataset, Cdataset (Luo et al., 2016), consists of 663 drugs registered in DrugBank, 409 diseases from the OMIM database, and 2532 known drug-disease associations. The third dataset, Ldataset (Yu et al., 2021), contains 18,416 drug-disease associations between 269 drugs and 598 diseases sourced from the Comparative Toxicogenomics Database(CTD) (Davis et al., 2023). The fourth dataset, LRSSL (Liang et al., 2017), comprises 763 drugs, 681 diseases, and 3051 validated drug-disease associations. Table 1 summarizes the four datasets' statistics.

This study determines drug similarity based on chemical structures obtained from DrugBank using standardized SMILES notation (Weininger, 1988). The Tanimoto score of the 2D chemical fingerprints of two drugs is then calculated using the chemistry development kit (Steinbeck et al., 2003). Disease similarity, on the other hand, is based on disease phenotypes and is computed using MimMiner (Van Driel et al., 2006). MimMiner gauges disease similarity by analyzing the similarity of MeSH terms in medical descriptions of diseases from the OMIM database (Lipscomb, 2000).

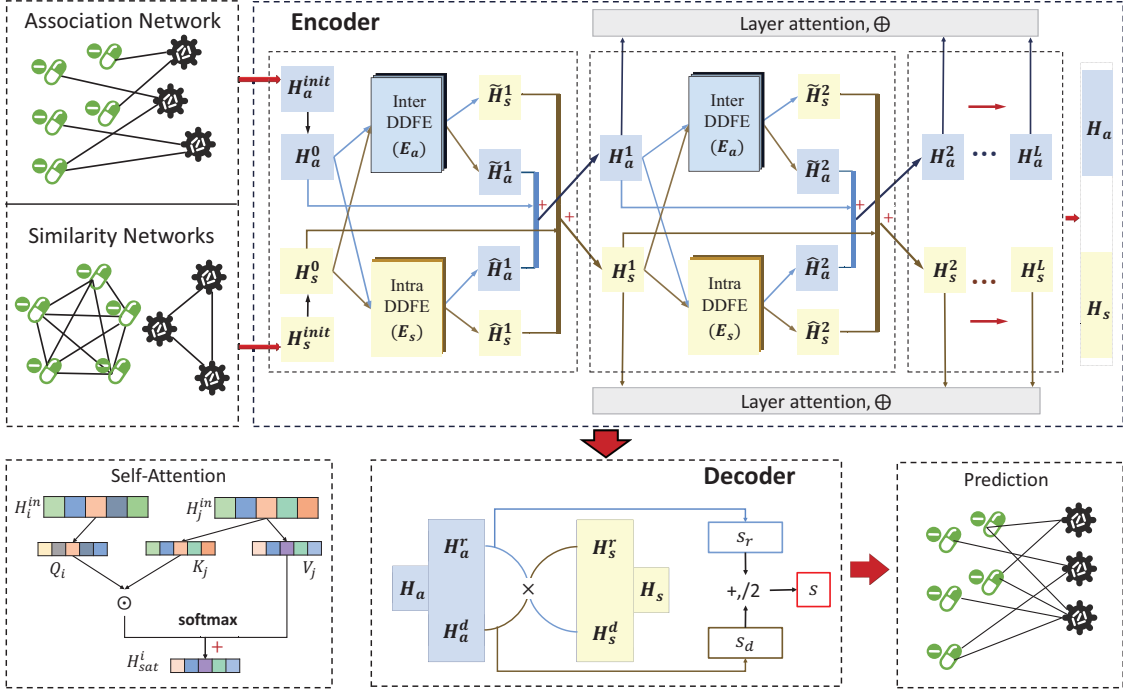


Figure 1: DFDRNN generates the similarity feature and the association feature for drugs and diseases based on established similarity networks and association networks. The encoding process utilizes a multi-layer connected network architecture, with each layer performing IntraDDFE and InterDDFE based on the self-attention mechanism. A layer attention mechanism is also introduced to compute the final similarity and association features. Finally, the decoder calculates drug-disease association scores by decoding separately for the drug and disease domains.

2.2. Model structure

Our research is focused on predicting potential associations between drugs and diseases. To this end, we proposed a dual-feature drug repositioning neural network (DFDRNN) model. The encoder of DFDRNN encompasses two dual-feature extraction modules: the intra-domain dual-feature extraction (IntraDDFE) module and the inter-domain dual-feature extraction (InterDDFE) module. While the IntraDDFE module extracts features among drugs (or diseases), the InterDDFE module extracts features between drugs and diseases and changes the features. A self-attention mechanism (SAM) model is employed when aggregating information to capture the complex relationship among adjacent nodes. The decoder of DFDRNN receives the results from the encoder and implements cross-dual-domain decoding, including both the drug and disease domains. Figure 1 illustrates the diagram of the proposed DFDRNN model.

2.2.1. Three networks

To illustrate the relationships among biological entities (drugs and diseases) and describe their feature, we establish three networks: the drug-drug similarity network, a weighted complete graph with a node-set representing the drugs, and the weight of each edge representing the degree of similarity between the two drugs incident with the edge; the disease-disease similarity network, a weighted complete graph with node set representing the diseases and the weight of each edge representing the degree of similarity of the two diseases

incident with the edge; and the drug-disease association network, a bipartite network with two parts representing the sets of drugs and diseases, respectively and each edge representing the associativity between the drug and diseases incident with the edge. We use three matrices to represent these three networks.

Specifically, suppose that there are n drugs (denoted by r_1, r_2, \dots, r_n) and m diseases (denoted by d_1, d_2, \dots, d_m). We use S^r (or S^d) to denote the adjacency matrix of a drug-drug similarity network (or disease-disease similarity network), which is an $n \times n$ ($m \times m$) real matrix such that the entry s_{ij}^r (or s_{ij}^d) $\in [0, 1]$ denotes the degree of similarity of drug i and drug j (or disease i and disease j), where $i, j \in \{1, 2, \dots, n\}$ (or $i, j \in \{1, 2, \dots, m\}$). For a drug-disease association network, we use a $n \times m$ binary matrix, denoted by A , to represent it, where the entry $a_{ij} = 1$ if drug i is associated with disease j and $a_{ij} = 0$ if drug i is not associated with disease j or the associativity is yet to be observed, for $i = 1, 2, \dots, n$ and $j = 1, 2, \dots, m$.

To reduce the impact of data noise, we aggregate only the top- t neighbors for each drug in S^r and each disease in S^d , and then two new matrices $R \in \mathbb{R}^{n \times n}$ and $D \in \mathbb{R}^{m \times m}$ are generated to replace S^r and S^d , respectively, where the entries r_{ij} ($i, j \in \{1, 2, \dots, n\}$) of R and d_{ij} ($i, j \in \{1, 2, \dots, m\}$) of D are defined as follows. For a drug r_i (and a disease d_i), we denote by $N_t(r_i)$ (and $N_t(d_i)$) the set of t -nearest neighbors of r_i in S^r (and d_i in S^d), i.e., the weight of edge $r_i x$ (and edge $d_i y$) for every $x \in N_t(r_i)$ (and every

$y \in N_t(d_i)$ is top- t among all neighbors of r_i (and d_i), and let $\tilde{N}_t(r_i) = N_t(r_i) \cup \{r_i\}$ (and $\tilde{N}_t(d_i) = N_t(d_i) \cup \{d_i\}$) be the extended t -nearest neighbors of r_i (and d_i).

$$r_{ij} = \begin{cases} 1, & \text{if } r_j \in \tilde{N}_t(r_i) \\ 0, & \text{otherwise} \end{cases} \quad d_{ij} = \begin{cases} 1, & \text{if } d_j \in \tilde{N}_t(d_i) \\ 0, & \text{otherwise} \end{cases} \quad (1)$$

Finally, to encode drugs and diseases simultaneously and distinguish IntraDDFE from InterDDFE, we construct two heterogeneous networks E_s and E_a based on the above matrices R , D , and A . E_s is used for IntraDDFE, while E_a is used for InterDDFE, defined as:

$$E_s = \begin{bmatrix} R & 0 \\ 0 & D \end{bmatrix} \quad E_a = \begin{bmatrix} 0 & A \\ A^T & 0 \end{bmatrix} \quad (2)$$

2.2.2. Self-attention mechanism

The self-attention mechanism (SAM) can be described as a process associated with three vectors, i.e., one query vector Q_i , some key vectors K_j , and some value vector V_j , which maps Q_i and a group of K_j - V_j pairs to a new output vector. The output of the attention is a weighted sum of V_j vectors, where the weight for each V_j is computed by taking the dot product of the Q_i with the corresponding K_j (Vaswani et al., 2017). In our IntraDDFE and InterDDFE modules, we use the multi-head SAM to aggregate neighbor information for drugs and diseases. We use the notation **sam** to represent the multi-head SAM mapping that involves two parameters E and H^{in} , where $E \in \{E_s, E_a\}$ and $H^{in} \in \mathbb{R}^{(n+m) \times k}$ is an input feature matrix with embedding dimension k . The specific implementation of **sam** can be described as follows:

$$Q = H^{in}w^Q, \quad K = H^{in}w^K, \quad V = H^{in}w^V \quad (3)$$

where $w^Q, w^K, w^V \in \mathbb{R}^{k \times k}$ are three trainable $k \times k$ real matrices. Clearly, Q , K , and V are $(n+m) \times k$ real matrices.

Each Q , K , and V is partitioned into p parts (called heads), denoted by Q^i, K^i , and V^i , $i = 1, 2, \dots, p$, and the dimension of each part (i.e., the number of columns) is $k' = k/p$. We use Q_i^q , K_i^q , and V_i^q to denote the feature of node i in Q^q , K^q , and V^q (i.e., the row vector corresponding to i), respectively. Let X^q be the q -th head of $X \in \{Q, K, V\}$. Then, the weight of aggregating neighbor information is calculated based on Q^q and K^q . Specifically, for a node i (drug or disease), the weight β_{ij}^q of i aggregating its neighbor j is defined as

$$\beta_{ij}^q = \frac{\exp(\frac{Q_i^q \odot K_j^q}{\sqrt{k'}})}{\sum_{z \in N(i)} \exp(\frac{Q_i^q \odot K_z^q}{\sqrt{k'}})} \quad (4)$$

where \odot represents the inner product of vectors, $N(i)$ is the set of neighbors of node i . We denote by **concat**(x_1, x_2, \dots, x_p

the concatenation operation of vectors x_1, x_2, \dots, x_p . Then, the result corresponding to node i obtained by the SAM mapping (i.e., the i -th row vector in **sam**(E, H^{in})), denoted by H_{sam}^i , can be described as

$$H_{\text{sam}}^i = \text{concat}(\sum_{j \in N(i)} \beta_{ij}^1 V_j^1, \sum_{j \in N(i)} \beta_{ij}^2 V_j^2, \dots, \sum_{j \in N(i)} \beta_{ij}^p V_j^p) \quad (5)$$

Moreover, let H_{sam} represent the feature matrix obtained by SAM, $H_r \in \mathbb{R}^{n \times k}$ be the drug feature obtained by SAM, and $H_d \in \mathbb{R}^{m \times k}$ is the disease feature obtained by SAM. Then, we have

$$H_r = \begin{bmatrix} H_{\text{sam}}^{r_1} \\ H_{\text{sam}}^{r_2} \\ \dots \\ H_{\text{sam}}^{r_n} \end{bmatrix}, \quad H_d = \begin{bmatrix} H_{\text{sam}}^{d_1} \\ H_{\text{sam}}^{d_2} \\ \dots \\ H_{\text{sam}}^{d_m} \end{bmatrix}, \quad H_{\text{sam}} = \begin{bmatrix} H_r \\ H_d \end{bmatrix} \quad (6)$$

A fully connected layer is applied after the SAM function to extract further features of drugs and diseases. We use the notation **samf** to denote the whole process, i.e., **samf** is the combination of **sam** with a fully connected (FC) layer. Let $w_r \in \mathbb{R}^{k \times k}$ and $w_d \in \mathbb{R}^{k \times k}$ be trainable parameter matrices, b_r and b_d be biases, and σ be a LeakyRELU (Maas et al., 2013) activation function. Then,

$$\begin{aligned} \text{samf}(E, H^{in}) &= \text{FC}(\text{sam}(E, H^{in})) \\ &= \begin{bmatrix} \sigma(H_r w_r + b_r) \\ \sigma(H_d w_d + b_d) \end{bmatrix} \end{aligned} \quad (7)$$

2.2.3. Encoder

The DFDRNN model is a multi-layer connected network architecture, where each layer involves two types of dual-feature extraction modules: IntraDDFE module based on network E_s and InterDDFE module based on network E_a . First, the initial features of drugs and diseases are generated in two features, including the similarity feature H_s^{init} and the association feature H_a^{init} , described as follows.

$$H_s^{init} = \begin{bmatrix} S^r & 0 \\ 0 & S^d \end{bmatrix} \quad H_a^{init} = \begin{bmatrix} 0 & A \\ A^T & 0 \end{bmatrix} \quad (8)$$

Next, DFDRNN projects the initial features to a k -dimensional space through a linear layer. The similarity feature H_s^0 and the association feature H_a^0 in the 0-layer are defined as follows:

$$H_s^0 = H_s^{init} \times M, \quad H_a^0 = H_a^{init} \times M \quad (9)$$

where $M \in \mathbb{R}^{(n+m) \times k}$ is trainable parameter matrix.

Now, we consider the process of extracting features in the ℓ -th layer for $\ell \geq 1$. In the ℓ -th layer, we denote by f^ℓ the IntraDDFE function in this layer, H_s^ℓ and H_a^ℓ

are the input similarity feature and the input association feature, respectively, $\hat{H}_s^{\ell+1}$ and $\hat{H}_a^{\ell+1}$ represent the obtained similarity feature and association feature by IntraDDFE, and samf_f^ℓ the aggregation function of ℓ -th layer for IntraDDFE. Then,

$$\begin{aligned} (\hat{H}_s^{\ell+1}, \hat{H}_a^{\ell+1}) &= f^\ell(E_s, H_s^\ell, H_a^\ell) \\ &= (\text{samf}_f^\ell(E_s, H_s^\ell), \text{samf}_f^\ell(E_s, H_a^\ell)) \end{aligned} \quad (10)$$

Since IntraDDFE extracts features within a single domain, the dual-feature does not undergo dynamic changes. Thus, the input similarity features H_s^ℓ produce the output similarity features $\hat{H}_s^{\ell+1}$, and the input association features H_a^ℓ produce the output association features $\hat{H}_a^{\ell+1}$. Next, we use g^ℓ to denote the InterDDFE function in the ℓ -th layer. Similarly, $\tilde{H}_s^{\ell+1}$ and $\tilde{H}_a^{\ell+1}$ represent the obtained similarity feature and association feature by InterDDFE, respectively, and samf_g^ℓ represents the aggregation function. Then,

$$\begin{aligned} (\tilde{H}_a^{\ell+1}, \tilde{H}_s^{\ell+1}) &= g^\ell(E_a, H_s^\ell, H_a^\ell) \\ &= (\text{samf}_g^\ell(E_a, H_s^\ell), \text{samf}_g^\ell(E_a, H_a^\ell)) \end{aligned} \quad (11)$$

Since the InterDDFE module extracts features across domains, dual-feature undergo dynamic changes. Specifically, the similarity feature H_s^ℓ is changed into the association feature $\tilde{H}_a^{\ell+1}$, and the association feature H_a^ℓ is changed into the similarity feature $\tilde{H}_s^{\ell+1}$.

Finally, for each module, the similarity (and association) features (including one input feature and two output features corresponding to the two modules) in the ℓ -layer are added into an input similarity (and association) feature of the $(\ell+1)$ -layer, i.e.,

$$H_s^{\ell+1} = \hat{H}_s^{\ell+1} + \tilde{H}_s^{\ell+1} + H_s^\ell \quad (12)$$

$$H_a^{\ell+1} = \hat{H}_a^{\ell+1} + \tilde{H}_a^{\ell+1} + H_a^\ell \quad (13)$$

As the depth of network layers increases, the valuable information for predicting drug-disease association extracted by the DFDRNN model decreases. Therefore, we introduce a layer attention mechanism to allocate different weights to the results of different layers. We use L to represent the total number of layers in DFDRNN. The weight of the ℓ -th layer, denoted by β^ℓ , is initialized by $1/L$ and automatically learned by the model. Then, the final encoding of the similarity feature and the association feature H_s^r , H_a^r , H_s^d , and H_a^d of drugs and diseases are obtained by implementing the layer attention mechanism as follows.

$$\begin{bmatrix} H_s^r \\ H_s^d \end{bmatrix} = \sum_{\ell=1}^L (\beta^\ell \times H_s^\ell), \quad \begin{bmatrix} H_a^r \\ H_a^d \end{bmatrix} = \sum_{\ell=1}^L (\beta^\ell \times H_a^\ell) \quad (14)$$

2.2.4. Decoder

A cross-dual-domain decoder is utilized to predict drug-disease association. We perform cross computation between two features, using $s_r \in \mathbb{R}^{n \times m}$ and $s_d \in \mathbb{R}^{n \times m}$ to represent the prediction values for the drug domain and the disease domain, respectively. Let $s \in \mathbb{R}^{n \times m}$ denote the final score matrix of drug-disease associations, where s_{ij} represents the prediction score between drug r_i and disease d_j . That is,

$$s_r = \text{sigmod}(H_a^r \times (H_s^d)^T) \quad (15)$$

$$s_d = \text{sigmod}(H_a^d \times (H_s^r)^T) \quad (16)$$

$$s = (s_r + (s_d)^T)/2.0 \quad (17)$$

Algorithm 1 gives a detailed explanation of predicting novel drug-disease associations using DFDRNN.

2.3. Optimization

Predicting the drug-disease association can be viewed as a binary classification task. The objective is to determine whether a given drug is associated with a specific disease. Given the serious imbalance between the number of positive samples (drug-disease associations) and negative samples (drug-disease non-associations), we employ binary cross-entropy as the loss function. We use y^+ and y^- to represent the positive and negative labels in the dataset, respectively. We use $\lambda = \frac{|y^-|}{|y^+|}$ to reduce the impact of this kind of data imbalance and denote by (i, j) a drug(r_i)-disease(d_j) pair in y^+ or y^- , where $|y^-|$ and $|y^+|$ represent the cardinalities of y^+ or y^- , respectively.

$$\text{loss} = -\frac{1}{n+m} (\lambda \times \sum_{(i,j) \in y^+} \log(s_{ij}) + \sum_{(i,j) \in y^-} \log(1-s_{ij})) \quad (18)$$

We optimize the DFDRNN model using the Adam (Kingma and Ba, 2014) optimizer and initialize the parameters' weights with Xavier initialization (Glorot and Bengio, 2010). We randomly drop some edges and apply regular dropout (Srivastava et al., 2014) to improve the model's generalization ability.

3. Experiments and Results

3.1. Baseline methods

To assess DFDRNN's performance, we compared it with six state-of-the-art drug-disease association prediction models across the above four datasets. These models are:

- LAGCN (Yu et al., 2021): This method utilizes multi-layer GCNs for neighbor information propagation on heterogeneous networks and introduces the layer attention mechanism.

- DRHGCN (Cai et al., 2021): This model uses GCN and bilinear aggregators to design inter-domain and intra-domain embeddings for predicting drug-disease associations.

- DRWBNCF (Meng et al., 2022): This model focuses on the interaction information between neighbors and uses

Algorithm 1 DFDRNN

```

1: Input: Two heterogeneous network ( $E_s$  and  $E_a$ ); initial the similarity feature and the association feature ( $H_s^{init}$  and  $H_a^{init}$ ); number of layers  $L$ ; maximum training epochs  $C$ .
2: Output: Drug-disease association score matrix  $s$ .
3: Initialize the weight matrix ( $w^Q, w^K, w^V, w_r, w_b, \dots$ ).
4: for  $c = 1$  to  $C$ 
5:   Compute the similarity feature  $H_s^0$  and the association feature  $H_a^0$  with Equation (9).
6:   for  $i = 1$  to  $L$ 
7:     Compute IntraDDFE  $\hat{H}_s^\ell, \hat{H}_a^\ell$  with Equation (10).
8:     Compute InterDDFE  $\tilde{H}_s^\ell, \tilde{H}_a^\ell$  with Equation (11).
9:     Fuse the same feature and the output of the previous layer yields  $H_s^\ell$  and  $H_a^\ell$  with Equation (12) (13)
10:    end for
11:    Utilizing layer attention mechanism to compute the final embedding with Equation (14)
12:    Obtain Computer the prediction score matrix  $s$  with Equation (15)(16)(17)
13:    Update the parameters  $w^Q, w^K, w^V, w_r, w_b, \dots$  with Equation (18).
14:     $c \leftarrow c + 1$ .
15: end for

```

generalized matrix factorization collaborative filtering to predict drug-disease associations.

- NCH-DDA (Zhang et al., 2024): This method involves the design of a single-neighborhood feature extraction module and a multi-neighborhood feature extraction module to extract features for drugs and diseases. Additionally, it introduces neighborhood contrastive learning for drug-disease association prediction.

- HDGAT (Huang et al., 2024): This approach combines graph convolutional neural networks with bidirectional extended short-term memory networks and integrates layer attention mechanisms and residual connections.

- DRGBCN (Tang et al., 2023): This method utilizes layer attention graph convolutional networks to encode drugs and diseases and employs bilinear attention network modules to enhance their intricate relationship.

3.2. Experimental parameter configuration

The model's parameter values are as follows: DFDRNN's feature embedding dimension is 128; the number of network layers is 3; the number of attention heads is $p = 2$; the dropout rate is 0.4; the edge dropout rate is 0.5 on the Ldataset and 0.2 on other datasets; the learning rate is 0.008; and the maximum training epoch is 800. Additionally, we set top- t to 7 based on parameter sensitivity experiments.

3.3. Evaluation metrics

We categorize the prediction results into four sets. As shown in Table 2, TP represents the number of true positives correctly classified as positive, FN represents the number of false negatives incorrectly classified as negative, FP represents the number of false positives incorrectly classified as positive, and TN represents the number of true negatives correctly classified as negative. We then calculate True Positive Rate (TPR or Recall), False Positive Rate (FPR), and precision as follows:

$$TPR(\text{or Recall}) = \frac{TP}{TP + FN} \quad (19)$$

Table 2
The statistics of the four sets used in this study

		Predicted	
		Positive	Negative
Actual	Positive	TP	FN
	Negative	FP	TN

$$FPR = \frac{FP}{FP + TN} \quad (20)$$

$$Precision = \frac{TP}{TP + FP} \quad (21)$$

Calculating the FPR, TPR, and precision at various thresholds, we construct the receiver operating characteristic (ROC) curve, with FPR on the X-axis and TPR on the Y-axis. Additionally, we generate the precision-recall (PR) curve, with recall on the X-axis and precision on the Y-axis. The evaluation metrics used for DFDRNN are the area under the ROC curve (AUROC) and the area under the PR curve (AUPR).

3.4. Performance of DFDRNN in the cross-validation

We employ the 10-fold cross-validation method to assess the model's performance. During this process, the dataset is randomly partitioned into ten mutually exclusive subsets, each containing 10% known drug-disease association pairs and 10% unknown pairs. One subset serves as the test set, while the remaining nine subsets are used to train the model. This process is repeated ten times (i.e., 10-fold cross-validation) with different random seeds, and the average and standard deviation of the results are calculated to compare the model's performance. The experimental results, including AUROC and AUPR values, are presented in Table 3. The

Table 3

The AUROCs and AUPRs of DFDRNN and the other comparative models under 10-times 10-fold cross-validation.

Metrics	Model	Fdataset	Cdataset	Ldataset	LRSSL	Avg.
AUROC	LAGCN	0.881±0.002	0.911±0.002	0.864±0.001	0.935±0.001	0.898
	DRHGCN	0.949±0.001	<u>0.965±0.001</u>	0.864±0.001	0.960±0.001	0.935
	DRWBNCF	0.924±0.002	0.942±0.001	0.821±0.001	0.935±0.001	0.906
	NCH-DDA	<u>0.954±0.002</u>	0.959±0.002	<u>0.879±0.001</u>	<u>0.963±0.002</u>	<u>0.939</u>
	HDGAT	0.917±0.002	0.939±0.001	0.874±0.001	0.936±0.001	0.916
	DRGBCN	0.931±0.003	0.946±0.001	0.824±0.002	0.943±0.001	0.911
	DFDRNN	0.960±0.001	0.973±0.001	0.885±0.001	0.965±0.001	0.946
AUPR	LAGCN	0.197±0.005	0.307±0.008	0.522±0.002	0.254±0.002	0.320
	DRHGCN	<u>0.531±0.003</u>	0.619±0.003	0.523±0.001	0.408±0.002	0.520
	DRWBNCF	0.493±0.001	0.569±0.004	0.413±0.003	0.349±0.005	0.456
	NCH-DDA	0.623±0.006	<u>0.675±0.003</u>	<u>0.552±0.002</u>	<u>0.466±0.002</u>	<u>0.579</u>
	HDGAT	0.505±0.005	0.566±0.008	0.546±0.003	0.403±0.005	0.505
	DRGBCN	0.408±0.007	0.451±0.006	0.434±0.005	0.262±0.006	0.388
	DFDRNN	0.623±0.003	0.688±0.002	0.573±0.001	0.502±0.002	0.597

The best results in each column are in bold faces and the second best results are underlined.

ROC and PR curves can also be found in Supplementary Figures S1-S4.

In Table 3, it is evident that DFDRNN outperformed all other models by achieving the highest average AUROC of 0.946 and the highest average AUPR of 0.597 across the four datasets. This performance surpassed the second-ranked NCH-DDA model by 0.75% and 3.1% in AUROC and AUPR, respectively. DFDRNN demonstrated the best AUROC and AUPR on all four datasets, showcasing its predictive solid capability for potential drug-disease associations based on known associations. It's worth mentioning that NCH-DDA performed exceptionally well, coming in second only to DFDRNN, which may be attributed to its feature extraction from different neighborhoods and the fusion of features using contrastive learning loss.

3.5. Effect of the number of nearest neighbors

In the context of DFDRNN, the value of top- t determines the number of neighbors features aggregated during IntraDDFE, which influences the model's performance. A small value of t limits the neighbor information obtained, thereby affecting the model's performance. On the other hand, as t increases, more neighbors are obtained, but this also introduces noise information, leading to the propagation of unnecessary data. The performance of DFDRNN under 10-fold cross-validation varies with t on the four datasets, as demonstrated in Figure 2 for $t \in \{1, 2, 3, \dots, 20\}$.

Based on the results shown in Figure 2 (a) and (b), DFDRNN performs the poorest across the four datasets when $t = 1$. However, as the t value increases, DFDRNN consistently maintains excellent performance, showcasing its remarkable stability, which can be credited to its robust self-attention mechanism's aggregation capability. Furthermore, the changes in average AUROC (Figure 2 (c)) and average AUPR (Figure 2 (d)) indicate that when $t = 7$, DFDRNN achieves the highest average AUROC of 0.9452 and the highest average AUPR of 0.5973 across the four datasets.

For detailed numerical values, please refer to Supplementary Tables S1 and S2.

3.6. Ablation analysis

3.6.1. Encoder

The encoder of DFDRNN incorporates SAM to encode drugs (or diseases) into the similarity feature (SF) and the association feature (AF). We introduce two dual-feature extraction modules, IntraDDFE and InterDDFE, to precisely encode drugs and diseases, with InterDDFE changing the feature (CF) of drugs (or diseases). We developed various model variants to underscore these elements' importance in the DFDRNN encoder and evaluated their performance.

- DFDRNN-SF: Remove the association feature and encode drugs and diseases solely as the similarity feature.
- DFDRNN-AF: Remove the similarity feature and encode drugs and diseases solely as the association feature.
- DFDRNN-GCN: SAM was replaced by a GCN to observe the impact on the model's performance.
- DFDRNN-noCF: Remove the change of features in InterDDFE, meaning that the similarity feature and the association feature will not be changed into each other after InterDDFE.

Table 4 presents the AUROC and AUPR values of DFDRNN and its four variants under 10-fold cross-validation. By comparing the two variants of DFDRNN, DFDRNN-SF and DFDRNN-AF, we observe that DFDRNN-SF performs better than DFDRNN-AF on the Fdataset, Cdataset, and LRSSL, indicating the contribution of the similarity feature is greater than that of the association feature on these three datasets. However, on the Ldataset, the contribution of the association feature is greater than that of the similarity

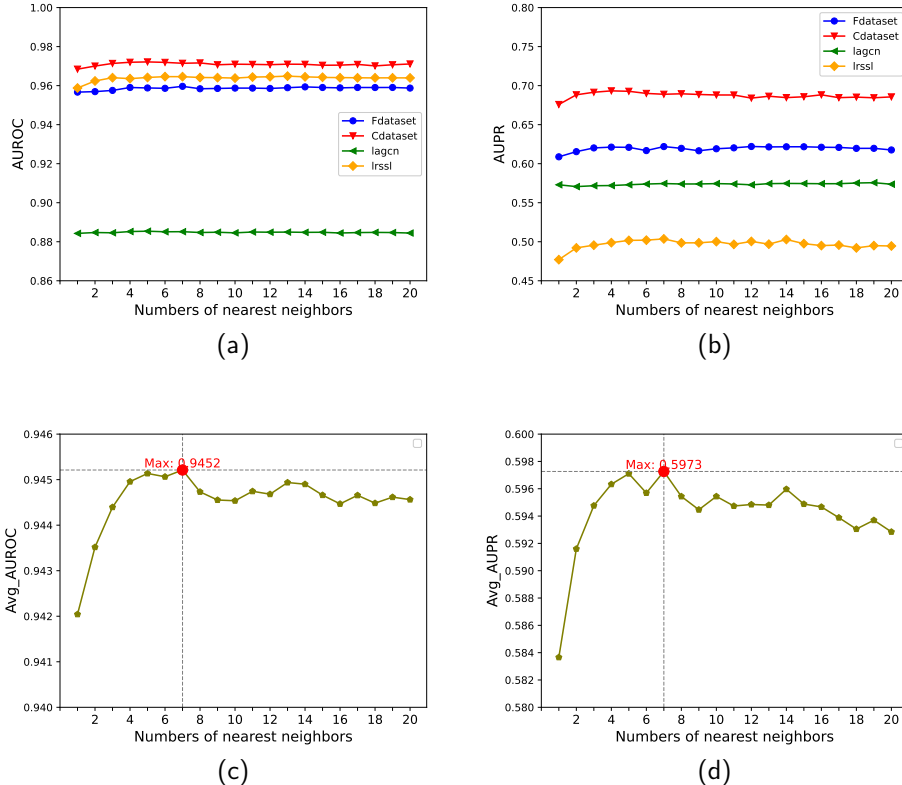


Figure 2: (a)Line plot of AUROC as a function of top- t on four benchmark datasets; (b)Line plot of AUPR as a function of top- t on four benchmark datasets; (c)Line plot of the average AUROC as a function of top- t on four datasets; (d)Line plot of the average AUPR as a function of top- t on four datasets.

Table 4

The AUROCs and AUPRs of DFDRNN and its four variants under 10-fold cross-validation

Variants	Fdataset		Cdataset		Ldataset		LRSSL	
	AUROC	AUPR	AUROC	AUPR	AUROC	AUPR	AUROC	AUPR
DFDRNN-SF	0.958	0.612	0.972	0.690	0.873	0.538	0.964	0.464
DFDRNN-AF	0.942	0.606	0.962	0.678	0.884	0.570	0.950	0.504
DFDRNN-GCN	0.950	0.620	0.964	0.671	0.874	0.551	0.956	0.483
DFDRNN-noCF	0.959	0.611	0.970	0.676	0.868	0.523	0.963	0.462
DFDRNN	0.960	0.622	0.973	0.689	0.885	0.572	0.965	0.504

feature. Compared to DFDRNN, simultaneously encoding both features can significantly improve the model's performance. Compared to DFDRNN, DFDRNN-GCN demonstrates a noticeable decrease in AUROC values, highlighting the strong performance of SAM in extracting neighbor information. Furthermore, compared to DFDRNN, DFDRNN-noCF shows a significant decrease in AUPR on the Fdataset, Cdataset, and LRSSL datasets, and performs the worst on the Ldataset, indicating the necessity of changing features in the InterDDFE module.

3.6.2. Decoder

To demonstrate the effectiveness of the cross-dual-domain decoder, an experiment was designed to compare the AUROC value and the AUPR value obtained by DFDRNN with those obtained by five variants of DFDRNN, labeled as s_r , s_d , s^{non} , s_r^{non} , and s_d^{non} . Here, s_r (Equation 15), s_d (Equation 16), and s^{non} represent the models derived from DFDRNN by substituting the cross-dual-domain decoder with a single drug-domain decoder, a single disease-domain decoder and a non-cross dual-domain decoder encompassing decoding results of both the drug and disease domains (as shown in Figure 3), respectively. Similarly, s_r^{non} and s_d^{non} are

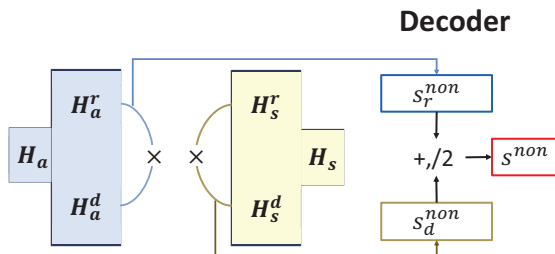


Figure 3: non-cross dual-domain decoder

models obtained from s_r^{non} by replacing the non-cross dual-domain decoder with a single drug-domain decoder and a single disease-domain decoder, respectively. The specific implementation of the non-cross dual-domain decoder is described as follows.

$$s_r^{\text{non}} = \text{sigmod}(H_a^r \times (H_a^d)^T) \quad (22)$$

$$s_d^{\text{non}} = \text{sigmod}(H_s^d \times (H_s^r)^T) \quad (23)$$

$$s^{\text{non}} = (s_r^{\text{non}} + (s_d^{\text{non}})^T) / 2.0 \quad (24)$$

The heatmaps, a crucial visual representation of the results, are shown in Figure 4 across the four datasets: Fdataset, Cdataset, Ldataset, and LRSSL. DFDRNN's consistent outperformance in achieving the highest AUROC and AUPR values across all four datasets underscores the significance of the cross-dual-domain decoder. Furthermore, the performance of s_r , s_d , s_r^{non} , and s_d^{non} consistently lags behind that of DFDRNN and s^{non} , further highlighting the effectiveness of dual-domain decoding.

3.7. Identification of candidates for new diseases

In late 2019, the discovery of COVID-19 presented a challenge in promptly researching and developing suitable drugs for treatment. Repurposing already approved drugs, such as remdesivir, favipiravir, and ribavirin, played a significant role in the timely control of the epidemic (Singh et al., 2020). Finding suitable drugs for emerging diseases is a complex and crucial task. To evaluate DFDRNN's predictive ability in identifying potential candidate drugs for new diseases, we conducted leave-one-out cross-validation (LOOCV) on the Fdataset dataset. Specifically, for each disease d_x , all drug-disease associations related to d_x were excluded from the analysis and treated as test samples. The remaining drug-disease associations were used as training samples, relying solely on the similarity between disease d_x and other diseases to predict its candidate drugs.

In Figure 5, the performance of DFDRNN in identifying potential drugs for new diseases on the Fdataset is illustrated. The experimental results show that DFDRNN achieved the highest AUROC of 0.8269, surpassing the second model NCH-DDA by 0.99%. Additionally, DFDRNN had the second-best performance in terms of AUPR, coming in behind only DRWBNCF.

Table 5
The top 10 DFDRNN-predicted candidate drugs for AD

Rank	Drug ID	Drug Name	Evidence
1	DB00915	Amantadine	DB/CTD/DrugCentral/ PubChem/ClinicalTrials
2	DB00564	Carbamazepine	CTD
3	DB04844	Tetrabenazine	CTD
4	DB00682	Warfarin	CTD
5	DB01241	Gemfibrozil	CTD/PubChem/ ClinicalTrials
6	DB00160	Alanine	CTD/ClinicalTrials
7	DB00903	Etacrynic acid	CTD
8	DB00928	Azacitidine	CTD
9	DB00482	Celecoxib	CTD
10	DB01262	Decitabine	CTD

3.8. Case study

To assess the real-world performance of DFDRNN, we conducted case studies on two diseases (Alzheimer's disease (AD) and Parkinson's disease (PD)) from the Fdataset. We utilized all drug-disease associations in the Fdataset as the training set to train DFDRNN and predict the association probabilities for all unknown drug-disease pairs. Subsequently, we ranked the drugs in descending order based on the association probabilities and obtained the top 10 predicted drugs for AD and PD. To confirm the accuracy of DFDRNN's predictions for AD and PD, we adopted highly reliable sources and clinical trials as references, including DB (Knox et al., 2024), PubChem (Kim et al., 2016), CTD (Davis et al., 2023), DrugCentral (Avram et al., 2021), and ClinicalTrials.

AD, the most prevalent form of progressive dementia in the elderly, is a neurodegenerative disorder. Table 5 displays the top 10 drugs predicted by DFDRNN for AD. Among these, Amantadine is the first drug predicted to hold therapeutic potential for AD. Amantadine, commonly used as an antiviral and antiparkinson drug, exhibits actions as an antiviral, antiparkinson, dopaminergic, and analgesic agent. It can also be utilized for the prevention or symptomatic treatment of influenza A. Previous studies have shown improvements in the mental state of two AD patients following Amantadine treatment (Erkulwater and Pillai, 1989). Carbamazepine functions as an anticonvulsant and analgesic drug. Earlier studies have suggested that the combined therapy of carbamazepine and haloperidol holds promise in the clinical management of elderly AD patients (Lemke, 1995). DFDRNN predicts an association with carbamazepine, which has been validated by CTD. Moreover, all the other drugs listed in Table 5 have been confirmed by relevant authoritative data sources, with a success rate of 100%.

Parkinson's disease (PD) is the second most common neurogenic disorder after AD. Table 6 presents the top 10 potential candidate drugs for PD predicted by DFDRNN. Among these candidates, Haloperidol, an antipsychotic agent, has been confirmed to be associated with PD by

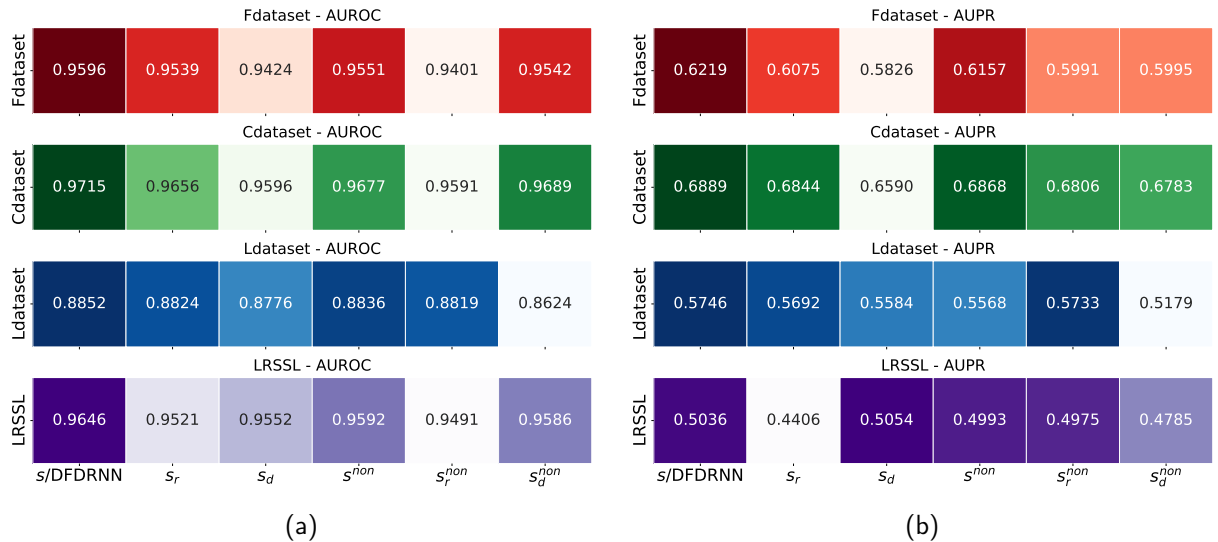


Figure 4: Performance of different decoding methods: (a) AUROC heatmap; (b) AUPR heatmap.

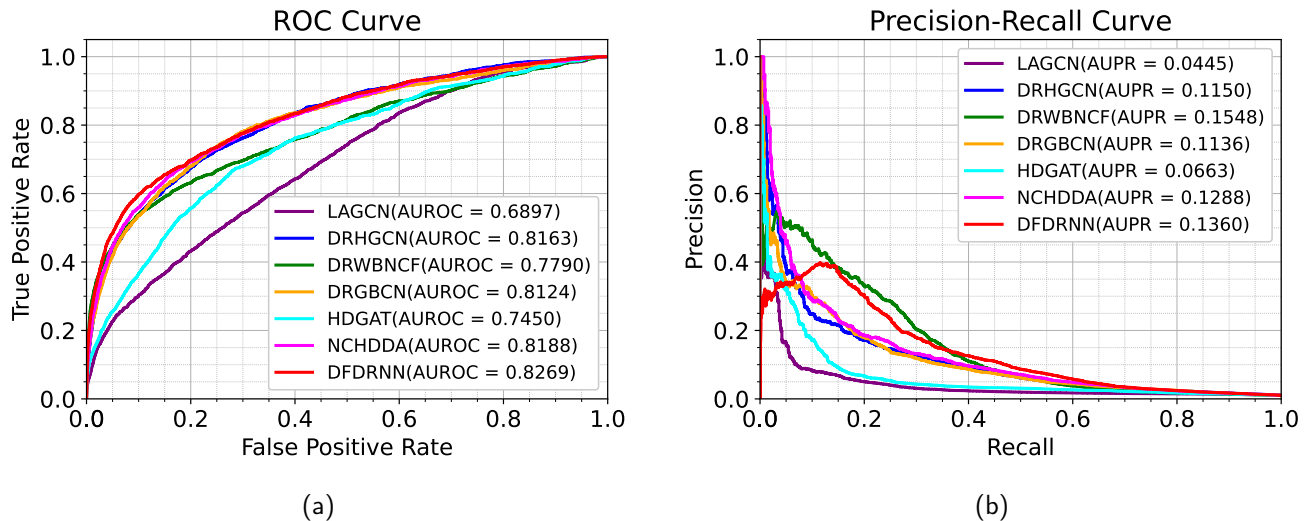


Figure 5: The performance of all methods in predicting potential drugs for new diseases on Fdataset: (a) Receiver operating characteristic (ROC) curves of prediction results obtained by applying DFDRNN and other competitive methods; (b) precision-recall (PR) curves of prediction results obtained by applying DFDRNN and other competitive methods.

DB, CTD, PubChem, and ClinicalTrials data sources. Additionally, Levodopa, a dopamine precursor used in PD management, has also been confirmed by multiple data sources. The fact that the predictions made by DFDRNN for the top 10 PD-related drugs have been validated by authoritative data sources provides reassurance about the reliability of the model.

4. Conclusion

Our study introduces DFDRNN, a neural network model designed for drug repositioning. DFDRNN uses IntraDDFE

and InterDDFE modules to extract the similarity and association features of drugs (or diseases), respectively, achieving precise encoding of drugs (or diseases). Compared with the IntraDDFE module, the InterDDFE module changes the similarity (or association) feature into the association (or similarity) feature. In both modules, we use the self-attention mechanism to aggregate the neighbor information of drugs (and diseases). Additionally, the DFDRNN model fuses three similarity (or association) features into a new similarity (or association) feature and uses a layer attention mechanism to calculate the final similarity (or association) feature. Finally, a cross-dual-domain decoder process is adopted

Table 6
The top 10 DFDRNN-predicted candidate drugs for PD

Rank	Drug ID	Drug Name	Evidence
1	DB00502	Haloperidol	DB/CTD/PubChem/ClinicalTrials
2	DB01068	Clonazepam	CTD/ClinicalTrials
3	DB01235	Levodopa	DB/CTD/DrugCentral/PubChem/ClinicalTrials
4	DB00810	Biperiden	DB/CTD/DrugCentral/PubChem
5	DB00424	Hyoscyamine	DB
6	DB00575	Clonidine	ClinicalTrials
7	DB00915	Amantadine	DB/DrugCentral/PubChem/ClinicalTrials
8	DB00989	Rivastigmine	DB/CTD/DrugCentral/PubChem/ClinicalTrials
9	DB00376	Trihexyphenidyl	DB/CTD/DrugCentral/PubChem
10	DB00215	Citalopram	CTD

to predict drug-disease associations in both the drug and disease domains. DFDRNN performs best in 10-fold cross-validation across four benchmark datasets and achieves the highest AUROC in leave-one-out cross-validation. The experimental results confirm the effectiveness of our proposed DFDRNN model in drug repositioning.

For future work, we would like to investigate whether specific enhancements, such as integrating temporal data and handling multi-modal data, could further enhance the performance of DFDRNN. By incorporating temporal data, the model can better understand and predict patterns over time. Integration of data from different modalities could provide a more comprehensive understanding of the input. We aim to identify and implement the appropriate techniques and models for these enhancements. Furthermore, we intend to explore the integration of additional biological entities, such as miRNA and proteins, for drug repositioning.

Acknowledgments

This work was supported by the National Key R&D Program of China (No. 2021ZD0112400) and the National Natural Science Foundation of China under grants 62172072 and 62272115.

References

- Avram, S., Bologa, C.G., Holmes, J., Bocci, G., Wilson, T.B., Nguyen, D.T., Curpan, R., Halip, L., Bora, A., Yang, J.J., et al., 2021. Drugcentral 2021 supports drug discovery and repositioning. *Nucleic acids research* 49, D1160–D1169. doi:<https://doi.org/10.1093/nar/gkaa997>.
- Bansal, C., Deepa, P., Agarwal, V., Chandra, R., 2024. A clustering and graph deep learning-based framework for covid-19 drug repurposing. *Expert Systems with Applications* 249, 123560. doi:<https://doi.org/10.1016/j.eswa.2024.123560>.
- Cai, L., Chu, J., Xu, J., Meng, Y., Lu, C., Tang, X., Wang, G., Tian, G., Yang, J., 2023. Machine learning for drug repositioning: Recent advances and challenges. *Current Research in Chemical Biology* , 100042doi:<https://doi.org/10.1016/j.crchbi.2023.100042>.
- Cai, L., Lu, C., Xu, J., Meng, Y., Wang, P., Fu, X., Zeng, X., Su, Y., 2021. Drug repositioning based on the heterogeneous information fusion graph convolutional network. *Briefings in bioinformatics* 22, bbab319. doi:<https://doi.org/10.1093/bib/bbab319>.
- Davis, A.P., Wiegers, T.C., Johnson, R.J., Sciaky, D., Wiegers, J., Mattingly, C.J., 2023. Comparative toxicogenomics database (ctd): update 2023. *Nucleic acids research* 51, D1257–D1262. doi:<https://doi.org/10.1093/nar/gkac833>.
- DiMasi, J.A., Feldman, L., Seckler, A., Wilson, A., 2010. Trends in risks associated with new drug development: success rates for investigational drugs. *Clinical Pharmacology & Therapeutics* 87, 272–277. doi:<https://doi.org/10.1038/clpt.2009.295>.
- Dudley, J.T., Deshpande, T., Butte, A.J., 2011. Exploiting drug–disease relationships for computational drug repositioning. *Briefings in bioinformatics* 12, 303–311. doi:<https://doi.org/10.1093/bib/bbr013>.
- Erkulwater, S., Pillai, R., 1989. Amantadine and the end-stage dementia of alzheimer's type. *Southern medical journal* 82, 550–554. doi:<https://doi.org/10.1097/00007611-198905000-00004>.
- Fisher Wilson, J., 2006. Alterations in processes and priorities needed for new drug development. doi:<https://doi.org/10.7326/0003-4819-145-10-200611210-00024>.
- Glorot, X., Bengio, Y., 2010. Understanding the difficulty of training deep feedforward neural networks, in: *Proceedings of the thirteenth international conference on artificial intelligence and statistics, JMLR Workshop and Conference Proceedings*. pp. 249–256.
- Gottlieb, A., Stein, G.Y., Ruppin, E., Sharan, R., 2011. Predict: a method for inferring novel drug indications with application to personalized medicine. *Molecular systems biology* 7, 496. doi:<https://doi.org/10.1038/msb.2011.26>.
- Gu, Y., Zheng, S., Yin, Q., Jiang, R., Li, J., 2022. Redda: Integrating multiple biological relations to heterogeneous graph neural network for drug-disease association prediction. *Computers in biology and medicine* 150, 106127. doi:<https://doi.org/10.1016/j.combiomed.2022.106127>.
- Hamosh, A., Scott, A.F., Amberger, J.S., Bocchini, C.A., McKusick, V.A., 2005. Online mendelian inheritance in man (omim), a knowledgebase of human genes and genetic disorders. *Nucleic acids research* 33, D514–D517. doi:<https://doi.org/10.1093/nar/gki033>.
- Huang, S., Wang, M., Zheng, X., Chen, J., Tang, C., 2024. Hierarchical and dynamic graph attention network for drug-disease association prediction. *IEEE Journal of Biomedical and Health Informatics* doi:<https://doi.org/10.1109/JBHI.2024.3363080>.
- Kim, S., Thiessen, P.A., Bolton, E.E., Chen, J., Fu, G., Gindulyte, A., Han, L., He, J., He, S., Shoemaker, B.A., et al., 2016. Pubchem substance and compound databases. *Nucleic acids research* 44, D1202–D1213. doi:<https://doi.org/10.1093/nar/gkv951>.
- Kingma, D.P., Ba, J., 2014. Adam: A method for stochastic optimization. *arXiv preprint arXiv:1412.6980*.
- Knox, C., Wilson, M., Klinger, C.M., Franklin, M., Oler, E., Wilson, A., Pon, A., Cox, J., Chin, N.E., Strawbridge, S.A., et al., 2024. Drugbank 6.0: the drugbank knowledgebase for 2024. *Nucleic Acids Research* 52, D1265–D1275. doi:<https://doi.org/10.1093/nar/gkad976>.
- Lemke, M.R., 1995. Effect of carbamazepine on agitation in alzheimer's inpatients refractory to neuroleptics. *The Journal of clinical psychiatry* 56, 354–357.
- Liang, X., Zhang, P., Yan, L., Fu, Y., Peng, F., Qu, L., Shao, M., Chen, Y., Chen, Z., 2017. Lrssl: predict and interpret drug–disease associations based on data integration using sparse subspace learning. *Bioinformatics* 33, 1187–1196. doi:<https://doi.org/10.1093/bioinformatics/btw770>.
- Lipscomb, C.E., 2000. Medical subject headings (mesh). *Bulletin of the Medical Library Association* 88, 265.
- Luo, H., Li, M., Wang, S., Liu, Q., Li, Y., Wang, J., 2018. Computational drug repositioning using low-rank matrix approximation and randomized algorithms. *Bioinformatics* 34, 1904–1912. doi:<https://doi.org/10.1093/bioinformatics/bty013>.
- Luo, H., Wang, J., Li, M., Luo, J., Peng, X., Wu, F.X., Pan, Y., 2016. Drug repositioning based on comprehensive similarity measures and bi-random walk algorithm. *Bioinformatics* 32, 2664–2671. doi:<https://doi.org/10.1093/bioinformatics/btw228>.

- Maas, A.L., Hannun, A.Y., Ng, A.Y., et al., 2013. Rectifier nonlinearities improve neural network acoustic models, in: Proc. icml, Atlanta, GA, p. 3.
- Mahdaddi, A., Meshoul, S., Belguidoum, M., 2021. Ea-based hyperparameter optimization of hybrid deep learning models for effective drug-target interactions prediction. *Expert Systems with Applications* 185, 115525. doi:<https://doi.org/10.1016/j.eswa.2021.115525>.
- Meng, Y., Lu, C., Jin, M., Xu, J., Zeng, X., Yang, J., 2022. A weighted bilinear neural collaborative filtering approach for drug repositioning. *Briefings in bioinformatics* 23, bbab581. doi:<https://doi.org/10.1093/bib/bbab581>.
- Meng, Y., Wang, Y., Xu, J., Lu, C., Tang, X., Peng, T., Zhang, B., Tian, G., Yang, J., 2024. Drug repositioning based on weighted local information augmented graph neural network. *Briefings in Bioinformatics* 25, bbad431. doi:<https://doi.org/10.1093/bib/bbad431>.
- Peng, L., Zhu, W., Liao, B., Duan, Y., Chen, M., Chen, Y., Yang, J., 2017. Screening drug-target interactions with positive-unlabeled learning. *Scientific reports* 7, 8087. doi:<https://doi.org/10.1038/s41598-017-08079-7>.
- Sadeghi, S., Lu, J., Ngom, A., 2022. A network-based drug repurposing method via non-negative matrix factorization. *Bioinformatics* 38, 1369–1377. doi:<https://doi.org/10.1093/bioinformatics/btab826>.
- Shi, H., Liu, S., Chen, J., Li, X., Ma, Q., Yu, B., 2019. Predicting drug-target interactions using lasso with random forest based on evolutionary information and chemical structure. *Genomics* 111, 1839–1852. doi:<https://doi.org/10.1016/j.ygeno.2018.12.007>.
- Singh, T.U., Parida, S., Lingaraju, M.C., Kesavan, M., Kumar, D., Singh, R.K., 2020. Drug repurposing approach to fight covid-19. *Pharmacological reports* 72, 1479–1508. doi:<https://doi.org/10.1007/s43440-020-00155-6>.
- Srivastava, N., Hinton, G., Krizhevsky, A., Sutskever, I., Salakhutdinov, R., 2014. Dropout: a simple way to prevent neural networks from overfitting. *The journal of machine learning research* 15, 1929–1958.
- Steinbeck, C., Han, Y., Kuhn, S., Horlacher, O., Luttmann, E., Willighagen, E., 2003. The chemistry development kit (cdk): An open-source java library for chemo-and bioinformatics. *Journal of chemical information and computer sciences* 43, 493–500. doi:<https://doi.org/10.1021/ci025584y>.
- Sun, X., Wang, B., Zhang, J., Li, M., 2022. Partner-specific drug repositioning approach based on graph convolutional network. *IEEE Journal of Biomedical and Health Informatics* 26, 5757–5765. doi:<https://doi.org/10.1109/JBHI.2022.3194891>.
- Tang, X., Zhou, C., Lu, C., Meng, Y., Xu, J., Hu, X., Tian, G., Yang, J., 2023. Enhancing drug repositioning through local interactive learning with bilinear attention networks. *IEEE Journal of Biomedical and Health Informatics* doi:<https://doi.org/10.1109/JBHI.2023.3335275>.
- Van Driel, M.A., Bruggeman, J., Vriend, G., Brunner, H.G., Leunissen, J.A., 2006. A text-mining analysis of the human genome. *European journal of human genetics* 14, 535–542. doi:<https://doi.org/10.1038/sj.ejhg.5201585>.
- Vaswani, A., Shazeer, N., Parmar, N., Uszkoreit, J., Jones, L., Gomez, A.N., Kaiser, Ł., Polosukhin, I., 2017. Attention is all you need. *Advances in neural information processing systems* 30. doi:<https://doi.org/10.48550/arXiv.1706.03762>.
- Vijayan, R., Kihlberg, J., Cross, J.B., Poongavanam, V., 2022. Enhancing preclinical drug discovery with artificial intelligence. *Drug discovery today* 27, 967–984. doi:<https://doi.org/10.1016/j.drudis.2021.11.023>.
- Wang, L., Lu, Y., Li, D., Zhou, Y., Yu, L., Mesa Eguiagaray, I., Campbell, H., Li, X., Theodoratou, E., 2024. The landscape of the methodology in drug repurposing using human genomic data: a systematic review. *Briefings in bioinformatics* 25, bbad527. doi:<https://doi.org/10.1093/bib/bbad527>.
- Weininger, D., 1988. Smiles, a chemical language and information system. 1. introduction to methodology and encoding rules. *Journal of chemical information and computer sciences* 28, 31–36. doi:<https://doi.org/10.1021/ci00057a005>.
- Xuan, P., Sun, C., Zhang, T., Ye, Y., Shen, T., Dong, Y., 2019. Gradient boosting decision tree-based method for predicting interactions between target genes and drugs. *Frontiers in genetics* 10, 459. doi:<https://doi.org/10.3389/fgene.2019.00459>.
- Yang, M., Wu, G., Zhao, Q., Li, Y., Wang, J., 2021. Computational drug repositioning based on multi-similarities bilinear matrix factorization. *Briefings in bioinformatics* 22, bbaa267. doi:<https://doi.org/10.1093/bib/bbaa267>.
- Yang, Y., Sun, Y., Li, F., Guan, B., Liu, J.X., Shang, J., 2023. Mgcnr: Prediction of disease-related mirnas based on multiple graph convolutional networks and random forest. *IEEE Transactions on Neural Networks and Learning Systems* doi:<https://doi.org/10.1109/TNNLS.2023.3289182>.
- Yu, B., Chen, C., Zhou, H., Liu, B., Ma, Q., 2020. Gtb-ppi: predict protein–protein interactions based on l1-regularized logistic regression and gradient tree boosting. *Genomics, Proteomics and Bioinformatics* 18, 582–592. doi:<https://doi.org/10.1016/j.gpb.2021.01.001>.
- Yu, J.L., Dai, Q.Q., Li, G.B., 2022. Deep learning in target prediction and drug repositioning: Recent advances and challenges. *Drug Discovery Today* 27, 1796–1814. doi:<https://doi.org/10.1016/j.drudis.2021.10.010>.
- Yu, Z., Huang, F., Zhao, X., Xiao, W., Zhang, W., 2021. Predicting drug–disease associations through layer attention graph convolutional network. *Briefings in bioinformatics* 22, bbaa243. doi:<https://doi.org/10.1093/bib/bbaa243>.
- Zhang, J., Li, C., Lin, Y., Shao, Y., Li, S., 2017. Computational drug repositioning using collaborative filtering via multi-source fusion. *Expert Systems with Applications* 84, 281–289. doi:<https://doi.org/10.1016/j.eswa.2017.05.004>.
- Zhang, P., Che, C., Jin, B., Yuan, J., Li, R., Zhu, Y., 2024. Nch-dda: Neighborhood contrastive learning heterogeneous network for drug–disease association prediction. *Expert Systems with Applications* 238, 121855. doi:<https://doi.org/10.1016/j.eswa.2023.121855>.
- Zhao, B.W., Hu, L., You, Z.H., Wang, L., Su, X.R., 2022. Hingrl: predicting drug–disease associations with graph representation learning on heterogeneous information networks. *Briefings in bioinformatics* 23, bbab515. doi:<https://doi.org/10.1093/bib/bbab515>.
- Enqiang Zhu is a Professor at Guangzhou University who specializes in researching biological network analysis, discrete optimization algorithms, graph theory and combinatorial optimization, and machine learning. He has been recognized as a Taishan Scholar (Young Expert) of Shandong province and as a Youth Talent in Guangzhou City. Additionally, he serves as a Youth Associate Editor for the Chinese Journal of Electronics and has published over 100 academic papers.
- Xiang Li is a Master student at Guangzhou University, with research interests including graph neural networks, bioinformatics, and deep learning.
- Chanjuan Liu received her Ph.D. degree from Peking University in 2016. She is a professor at Dalian University of Technology. Her research interests include intelligent decision-making and optimization. She has authored over 60 papers published in journals, including IEEE Transactions on Neural Networks and Learning Systems and IEEE Transactions on Cybernetics. She has been chosen for the Youth Talent Support Project of the Chinese Association for Science and Technology.
- Nikhil R. Pal is a Professor of Techno India University. He was a professor of the Indian Statistical Institute (ISI) and founding Head of the Center for Artificial Intelligence and Machine Learning at ISI. His current research interest includes brain science, computational intelligence, machine learning and data mining. He was the Editor-in-Chief of the IEEE Transactions on Fuzzy Systems from January 2005–December 2010. He is a Fellow of the National Academy of Sciences, India, Indian National Academy of Engineering, Indian National Science Academy, and a Fellow of the IEEE.